



Research paper

Reactivity of $[\text{Pt}_2(\mu\text{-S})_2(\text{PPh}_3)_4]$ towards activated aliphatic bromoacyl electrophiles: Formation of mono-, homodi-, heterodi- and intramolecular-bridged alkylated products



Oguejifo T. Ujam^{a,b,*}, Eric Janusson^b, Rhonda Stoddard^b, J. Scott McIndoe^b, Allen G. Oliver^c, Paschal C. Odo^a, Ogbonna C. Ogbonna^a

^a Department of Pure and Industrial Chemistry, University of Nigeria, Nsukka 410001, Enugu State, Nigeria

^b Department of Chemistry, University of Victoria, P. O. Box 3065, Victoria, BC V8W 3V6, Canada

^c Department of Chemistry and Biochemistry, University of Notre Dame, Notre Dame, IN 46556, USA

ARTICLE INFO

Article history:

Received 9 March 2016

Received in revised form 13 April 2016

Accepted 11 May 2016

Available online 18 May 2016

Keywords:

Mass spectrometry

Alkylation

Platinum(II) complexes

X-ray crystallography

ABSTRACT

Reactions of $[\text{Pt}_2(\mu\text{-S})_2(\text{PPh}_3)_4]$ with activated aliphatic bromoacyl alkylating agents $\text{BrCH}_2\text{C}(\text{O})\text{C}(\text{CH}_3)_3$, $\text{BrCH}_2\text{C}(\text{O})\text{CH}_2\text{CH}_3$ and $\text{BrCH}_2\text{C}(\text{O})\text{C}(\text{O})\text{CH}_2\text{Br}$, were investigated by electrospray ionization mass spectrometry (ESI-MS) in real time using pressurized sample infusion (PSI). The laboratory scale reactions gave the mono-, dicationic and bridged, μ -thiolate complexes $[\text{Pt}_2(\mu\text{-S})\{\mu\text{-SCH}_2\text{C}(\text{O})\text{C}(\text{CH}_3)_3\}(\text{PPh}_3)_4]^+$, $[\text{Pt}_2\{\mu\text{-SCH}_2\text{C}(\text{O})\text{CH}_2\text{CH}_3\}_2(\text{PPh}_3)_4]^{2+}$ and $[\text{Pt}_2\{\mu\text{-SCH}_2\text{C}(\text{O})\text{C}(\text{O})\text{CH}_2\text{S}\}(\text{PPh}_3)_4]^{2+}$. Sequential reactions of $[\text{Pt}_2(\mu\text{-S})_2(\text{PPh}_3)_4]$ with $\text{BrCH}_2\text{C}(\text{O})\text{C}(\text{CH}_3)_3$ and $\text{BrCH}_2\text{C}(\text{O})\text{CH}_2\text{CH}_3$ yielded the heterodialkylated complex $[\text{Pt}_2\{\mu\text{-SCH}_2\text{C}(\text{O})\text{C}(\text{CH}_3)_3\}\{\mu\text{-SCH}_2\text{C}(\text{O})\text{CH}_2\text{CH}_3\}(\text{PPh}_3)_4]^{2+}$. The products were isolated as the $[\text{BPh}_4]^-$ or $[\text{PF}_6]^-$ salts and characterized by ESI-MS, IR, ^1H and ^{31}P NMR spectroscopy and single-crystal X-ray crystallography.

© 2016 Elsevier B.V. All rights reserved.

1. Introduction

The exceptional reactivities of the electron-rich bridging sulfide centers in the metalloligand, $[\text{Pt}_2(\mu\text{-S})_2(\text{PPh}_3)_4]$, **1** towards metal fragments have been documented in the formation of multimetallic aggregates of main group elements [1–4], transition metals [1,4–9] and uranium [10]. Similar chemistry has been reported for selenium analogue [11,12] and closely related complexes with different terminal phosphine ligands [13–15]. $[\text{Pt}_2(\mu\text{-S})_2(\text{PPh}_3)_4]$ is also known to react with mild alkylating agents such as $\text{CHCl}_3/\text{CH}_2\text{Cl}_2$ [16] and $\text{PhCH}_2\text{Br}/\text{MeI}$ [17] since it was first synthesized in 1971 [17]. There has been an evolving interest in the reactions of **1** towards organic electrophiles as a facile route to a variety of functionalized thiolate ligands [18,19]. The potential application of **1** for activation of carbon–halogen bonds [20,21] and as a template for generation of organochalcogen molecules has been described [22]. The conversion of one of the μ -sulfide ligands in **1** through monoalkylation to produce μ -thiolate species of the type $[\text{Pt}_2(\mu\text{-S})(\mu\text{-SR})(\text{PPh}_3)_4]^+$ has previously been explored under

ESI-MS conditions [18]. This resulted in laboratory macroscale synthesis of previously unknown monoalkylated thiolate complexes of **1**, incorporating diverse functionalities, where R contains a ketone, ester, amide, semicarbazone, thiosemicarbazone, oxime, guanidine, urea, thiourea nitrile [23] or fluorinated moiety [24]. Particularly significant is the fact that any desired organic group can be incorporated into **1** through monoalkylation with suitable electrophile. The monoalkylated derivative can also act as cationic metalloligand towards metal fragment [25,26].

Double alkylation of both sulfur atoms on the metalloligand has remained largely undeveloped because the nature of electrophile and other factors that encourage dialkylation of **1** is not well understood and therefore require further investigation. Upon monoalkylation, the nucleophilicity of the unsubstituted sulfide center is reduced, limiting double alkylation to only very strong electrophiles [19,27,28]. Earlier reports seem to suggest that the outcome of reaction of **1** with an electrophile is dependent on both the nature of the leaving group and conjugated aromatic parent fragment [19,27,28]. Synthesis of $[\text{Pt}_2(\mu\text{-SCH}_3)_2(\text{PPh}_3)_4](\text{PF}_6)_2$ **2** [19], from the reaction of **1** with dimethylsulfate, $(\text{Me})_2\text{SO}_4$, **3** was the first stable homodialkylated product with a non-halide leaving group $[\text{MeSO}_4]^-$. We have reported the isolation of $[\text{Pt}_2(\mu\text{-SCH}_2\text{C}(\text{O})\text{Ph})_2(\text{PPh}_3)_4](\text{PF}_6)_2$ **4** [28], from the reaction **1** with 2-bromoacetophenone, $\text{BrCH}_2\text{C}(\text{O})\text{Ph}$, **5** with bromide ion as the

* Corresponding author at: Department of Pure and Industrial Chemistry, University of Nigeria, Nsukka 410001, Enugu State, Nigeria. Tel.: +234 8062573097.

E-mail address: oguejifo.ujam@unn.edu.ng (O.T. Ujam).

leaving group. Monoalkylated complex, $[\text{Pt}_2(\mu\text{-S})(\mu\text{-SR})(\text{PPh}_3)_4]^+$ can further react with a very strong electrophile, **3** or **5** to yield a heterodiallylated complex of the type $[\text{Pt}_2\{\mu\text{-SR}'\}(\mu\text{-SR})(\text{PPh}_3)_4]^{2+}$ ($\text{R} = \text{any electrophile}$ and $\text{R}' = \text{CH}_2\text{C}(\text{O})\text{Ph}$ or CH_3) [19,28]. However, heterodiallylation of **1** that involve nucleophilic leaving group (e.g. Cl^- , Br^- and I^-) may result in the displacement of the terminal PPh_3 ligands to form complexes such as $[\text{Pt}_2\{\mu\text{-SCH}_2\text{C}(\text{O})\text{Ph}\}(\mu\text{-SR})(\text{PPh}_3)_3\text{Br}]^+$ ($\text{R} = \text{Et}$, Bu), $[\text{Pt}_2\{\mu\text{-SCH}_3\}_2(\text{PPh}_3)_3\text{I}]^+$ [18] and $[\text{Pt}_2\{\mu\text{-SCH}_3\}_2(\text{PPh}_3)_3\text{I}_2]$ [29] or expansion of the normally robust four-membered $\{\text{Pt}_2(\mu\text{-S})_2\}$ core [30]. However, careful visualization of the reaction and modification of the conditions may eliminate formation of unwanted products. We recently reported the reverse of the PPh_3 halide displacement [28] and the expansion of the $\{\text{Pt}_2(\mu\text{-S})_2\}$ core from the rearrangement of a four-membered ring bridged derivative, $[\text{Pt}_2\{\mu\text{-SCH}_2\text{C}(\text{O})\text{CH}_2\text{S}\}(\text{PPh}_3)_4]^{2+}$ to a five-membered ring $[\text{Pt}_2\{\mu\text{-SCH}_2\text{C}(\text{O})\text{CHS}\}(\text{PPh}_3)_4]^+$ with no PPh_3 displacement [30].

Manual injection of the reaction solution of **1** and an electrophile into ESI-MS from a reaction flask or vial involve mere screening of the species formed after longer interval of time and not monitoring of reaction progress and the formation of species in real time. Real time reaction visualization of chemical reaction [31] could be applied in characterisation of the formation of products and other species in the reaction of **1** with alkylating agents and help in eliminating undesired side reactions, improve isolation of target product, determine the reaction mechanism and allow for the acquisition of kinetic information on the reaction. To date kinetic analysis has not previously been applied in the investigation of the synthetic complexities surrounding the double alkylation of **1**. Consequently, the only reported electrophiles that are able to homodi- and heterodiallylate **1** are $\text{BrCH}_2\text{C}(\text{O})\text{Ph}$ and Me_2SO_4 . Among the few electrophiles that are able to dialkylate **1**, there is no clear similarities. In this contribution, we report on the micro-synthetic investigation of the reactivity of **1** towards the activated bromoacyl aliphatic alkylating agents with closely related functionalities and the rates of formation of mono-, homodi- and bridging di-alkylated derivatives using the pressurized sample infusion electrospray ionization mass spectrometry (PSI-ESI-MS) technique. Importantly, this leads to further understanding of the conditions that encourage the double alkylation of **1** and these insights have been applied to allow rational modification of the laboratory scale synthesis of novel μ -thiolate derivatives of **1**.

2. Results and discussion

2.1. Kinetic profile, synthesis and characterizations

In the development of the chemistry of **1**, electrospray ionization mass spectrometry (ESI-MS) has been a valuable tool. It is a robust, fast, highly sensitive technique, able to detect molecular masses at a wide range of minute concentrations, and achieve great accuracy due to its dynamic range. It is well-suited to the analysis of organometallics and coordination compounds because it is a “soft” ionization method, the molecular ion is easily discerned and fragmentation is minimal [32]. Pressurized sample infusion (PSI) is a real-time sample infusion technique for ESI-MS that was employed in this project which allows for the immediate visualization of the formation of products and for the kinetic information regarding their formation to be obtained [31,33,34]. This technique is analogous to a cannula transfer, in which the reacting solution is transferred through PEEK tubing directly into the ionizing source of the ESI-MS, through overpressure of the Schlenk flask with inert gas. ESI-MS has the advantage over other techniques for the efficient separation of complex reaction mixtures and contin-

uous monitoring of each charged species over time intervals of seconds, minutes to hours. The acquisition of each spectrum can take less than a second and each spectrum is then combined into a series of abundance traces. The shape of each trace provides a detailed kinetic profile for each species.

The kinetic profiles of the reactions of minuscule amounts of $[\text{Pt}_2(\mu\text{-S})_2(\text{PPh}_3)_4]$, **1** towards the electrophiles $\text{BrCH}_2\text{C}(\text{O})\text{C}(\text{CH}_3)_3$, **a**, $\text{BrCH}_2\text{C}(\text{O})\text{CH}_2\text{CH}_3$, **b**, and $\text{BrCH}_2\text{C}(\text{O})\text{C}(\text{O})\text{CH}_2\text{Br}$, **c**, in methanol were monitored by PSI-ESI-MS to determine the species formed, rate of reaction and completion time. A methanolic solution of **1** was transferred by PSI into ESI-MS. As soon as the signal for the mass of $[\mathbf{1}+\text{H}]^+$ appeared at $m/z = 1503.5$, $\text{BrCH}_2\text{C}(\text{O})\text{C}(\text{CH}_3)_3$, **a**, was added to the reaction solution through a syringe. There was a fast but steady decrease in the intensity of the $m/z = 1503.5$ peak and steady increase in the peak at $m/z = 1603.9$ for the monoalkylated product, $[\text{Pt}_2(\mu\text{-S})(\mu\text{-SCH}_2\text{C}(\text{O})\text{C}(\text{CH}_3)_3)(\text{PPh}_3)_4]^+$, **1a**. No double alkylation of **1** by **a** was observed under ESI-MS conditions, presumably due to the deactivating effect of the electron donating methyl groups of the pinacolone moiety on the alkylating carbon of $-\text{CH}_2\text{Br}$ group. Fig. 1 shows the ESI-MS plot of the reaction progress. Formation of the monoalkylated product, **1a**, was complete after 2 min as indicated by the disappearance of the $m/z = 1503.5$ peak. The monoalkylated complex was isolated from the laboratory scale reaction as the $[\text{BPh}_4]^-$ salt, $[\text{Pt}_2(\mu\text{-S})(\mu\text{-SCH}_2\text{C}(\text{O})\text{C}(\text{CH}_3)_3)(\text{PPh}_3)_4]^+[\text{BPh}_4]^-$, **1a**· BPh_4 as a yellow precipitate following filtration and the addition of excess NaBPh_4 and shown by positive ion mode ESI-MS as pure **1a**. Further stirring of the laboratory scale reaction for 24 h at 50 °C did not give any dialkylated product. **1a**· BPh_4 contains two nonequivalent phosphorus centers (thiolate and sulfide). The $^{31}\text{P}\{^1\text{H}\}$ NMR spectrum shows two different resonances at δ 23.39 and δ 23.90 and well-separated satellite peaks due to ^{195}Pt coupling, $^1J(\text{PtP}_\text{B})$ 3376 Hz and $^1J(\text{PtP}_\text{A})$ 2653 Hz respectively, consistent with unsymmetrical monoalkylated **1**. The coupling constants are due to the differing *trans* influence [35] of the thiolate versus sulfide ligand, with phosphines *trans* to the higher *trans*-influence sulfide showing a coupling constant of 2653 Hz while those *trans* to thiolate show 3376 Hz. The ^1H NMR spectrum shows resonances at δ 3.46 and 0.66 which were assigned to CH_2 and CH_3 groups respectively and complicated signals in the phenyl region due to the terminal PPh_3 groups. The IR spectra of **1a**· BPh_4 showed absorption peaks at 1708 cm^{-1} , characteristic of the carbonyl ($-\text{C}=\text{O}$) group of the incorporated electrophile.

The same technique employed in the reaction of **a** and **1** above was used to profile the reaction of **1** with $\text{BrCH}_2\text{C}(\text{O})\text{CH}_2\text{CH}_3$, **b**. Fig. 2 shows the reaction profile. The monoalkylation was fast and complete formation of $[\text{Pt}_2(\mu\text{-S})(\mu\text{-SCH}_2\text{C}(\text{O})\text{CH}_2\text{CH}_3)(\text{PPh}_3)_4]^+$, **1b** occurred in 6 min followed by slower dialkylation to give $[\text{Pt}_2(\mu\text{-SCH}_2\text{C}(\text{O})\text{CH}_2\text{CH}_3)_2(\text{PPh}_3)_4]^{2+}$, **1c**. The reaction completed in 100 min with the total consumption of the monoalkylated species. The rate of alkylation of the free sulfide in the monoalkylated complex, **1a** was slower than the monoalkylation of **1** as expected, due to the positive charge on the monoalkylated complex and steric shielding of the residual free sulfide ligand by the incorporated group. The dialkylated product was isolated in the laboratory synthesis after stirring for 2 h to complete the reaction as the hexafluorophosphate salt, **1c**· $(\text{PF}_6)_2$; by addition of excess NH_4PF_6 . Scheme 1 summarizes the reaction of **1** with these reactive electrophiles. The $^{31}\text{P}\{^1\text{H}\}$ NMR spectrum of **1c**· $(\text{PF}_6)_2$ showed a single resonance at δ 19.17, well-separated satellite peaks due to ^{195}Pt coupling and $^1J(\text{PtP})$ 3059 Hz, which is in agreement with the symmetrical nature of the complex. The ^1H NMR spectrum shows complicated signals around the phenyl region but also indicated distinct broad resonances at δ 2.58, δ 1.88 and δ 0.72 assigned to protons of the two $-\text{SCH}_2-$, $-\text{CH}_2-$ and $-\text{CH}_3$ groups respectively. The X-ray structure of **1c** was determined and the molecular structure of the core shown in Fig. 4. The selected bond

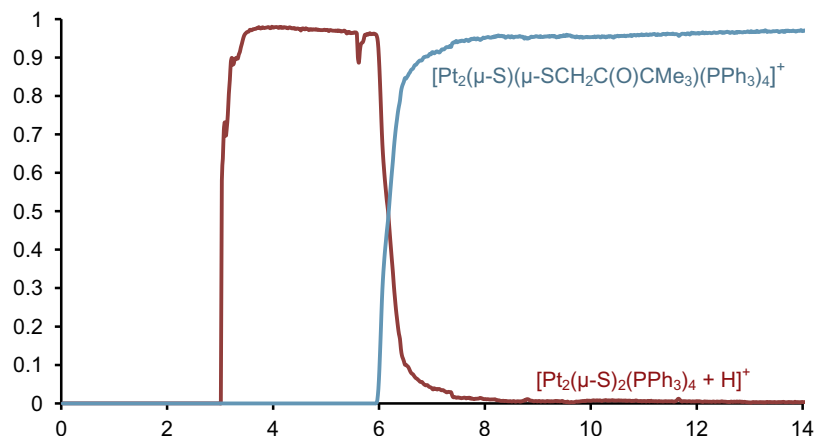


Fig. 1. The profile of the reaction of $[\text{Pt}_2(\mu\text{-S})_2(\text{PPh}_3)_4]$ (injected at 3 min) with $\text{BrCH}_2\text{C}(\text{O})\text{CMe}_3$ (injected at 6 min) to form the monocation $[\text{Pt}_2(\mu\text{-S})(\mu\text{-SCH}_2\text{C}(\text{O})\text{CMe}_3)(\text{PPh}_3)_4]^+$, **1a**. Traces are normalized to the total ion current.

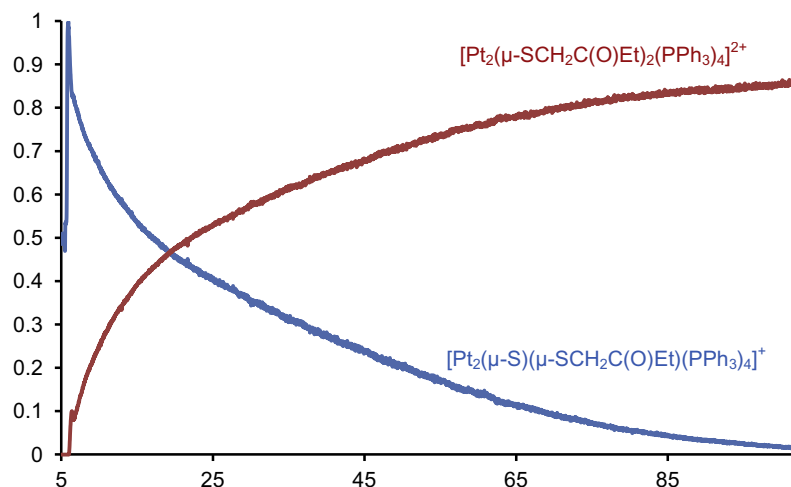


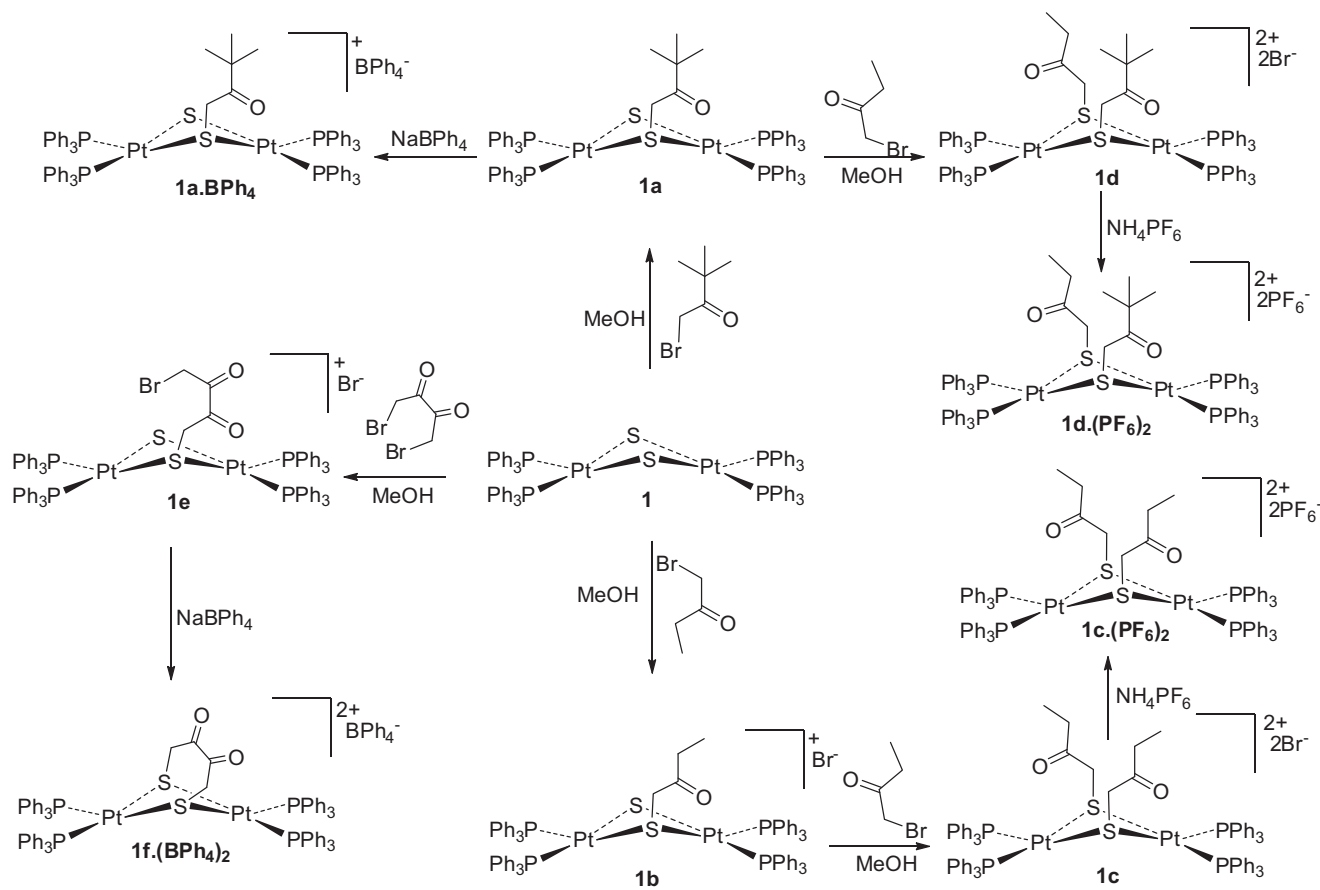
Fig. 2. The profile of the reaction of $\text{Pt}_2(\mu\text{-S})_2(\text{PPh}_3)_4$ with excess $\text{BrCH}_2\text{C}(\text{O})\text{CH}_2\text{CH}_3$ (injected at ~ 4 min) to form first the monocation $[\text{Pt}_2(\mu\text{-S})(\mu\text{-SCH}_2\text{C}(\text{O})\text{CH}_2\text{CH}_3)(\text{PPh}_3)_4]^+$, **1b** then the dication $[\text{Pt}_2(\mu\text{-SCH}_2\text{C}(\text{O})\text{CH}_2\text{CH}_3)_2(\text{PPh}_3)_4]^{2+}$, **1c**.

lengths and angles are given in Table 1. The $\{\text{Pt}_2(\mu\text{-S})_2\}$ core of **1c**· $(\text{PF}_6)_2$ has a dihedral angle, θ , of 159.82° between the two PtS_2 planes, which is considerably flatter when compared with the corresponding angles in $[\text{Pt}_2(\mu\text{-SCH}_3)_2(\text{PPh}_3)_4]^{2+}$ (156.87°) [19], $[\text{Pt}_2(\mu\text{-SCH}_2\text{C}(\text{O})\text{Ph})_2(\text{PPh}_3)_4]^{2+}$ (156.36°) [28]. The IR spectra of **1c**· $(\text{PF}_6)_2$ showed absorption peaks at 1712 cm^{-1} attributable to the incorporated carbonyl ($>\text{C}=\text{O}$) groups of the electrophile.

Exceptionally strong alkylating agents like $(\text{Me})_2\text{SO}_4$ and $\text{PhC}(\text{O})\text{CH}_2\text{Br}$ are notably able to alkylate the free sulfide in monoalkylated derivatives of the type $[\text{Pt}_2(\mu\text{-S})(\mu\text{-SR})(\text{PPh}_3)_4]^+$, generating mixed thiolate complexes [19,28]. The ability of $\text{BrCH}_2\text{C}(\text{O})\text{CH}_2\text{CH}_3$, **b** to double alkylate **1** indicates it is a stronger electrophile than $\text{BrCH}_2\text{C}(\text{O})\text{C}(\text{CH}_3)_3$, **a** and suggested it could further alkylate the unsubstituted sulfide in **1a**. In order to investigate this, a combination of the ESI-MS predetermined reaction times and conditions of the reactions of the two alkylating agents, **1a** and **1b** with **1** were strictly employed because prolonged stirring or elevated temperatures encourage undesired side reaction like the displacement of the terminal triphenyl phosphine ligands by the Br^- leaving species [28]. First, monoalkylated complex $[\text{Pt}_2(\mu\text{-S})(\mu\text{-SCH}_2\text{C}(\text{O})\text{C}(\text{CH}_3)_3)(\text{PPh}_3)_4]^+$, **1a** was generated *in situ* by reacting 1:1 mol equivalent of $\text{BrCH}_2\text{C}(\text{O})\text{C}(\text{CH}_3)_3$ and $[\text{Pt}_2(\mu\text{-S})_2(\text{PPh}_3)_4]$ and as soon as the formation of the monoalkylated complex was completed, excess $\text{BrCH}_2\text{C}(\text{O})\text{CH}_2\text{CH}_3$ was added to the reaction mixture. The

reaction completed after an hour to give only the heterodialkylated complex $[\text{Pt}_2(\mu\text{-SCH}_2(\text{O})\text{CH}_2\text{CH}_3)(\mu\text{-SCH}_2\text{C}(\text{O})\text{C}(\text{CH}_3)_3)(\text{PPh}_3)_4]^{2+}$, **1d** which was subsequently isolated as the $[\text{PF}_6]^-$ salt, $[\text{Pt}_2(\mu\text{-SCH}_2(\text{O})\text{CH}_2\text{CH}_3)(\mu\text{-SCH}_2\text{C}(\text{O})\text{C}(\text{CH}_3)_3)(\text{PPh}_3)_4](\text{PF}_6)_2$, **1d**· $(\text{PF}_6)_2$. The $^3\text{1P}\{^1\text{H}\}$ NMR of **1d**· $(\text{PF}_6)_2$ showed two well-separated resonance signals at δ 18.62 and δ 19.28 with a corresponding $^1\text{J}(\text{PtP})$ of 3078 Hz and 3082 Hz, for $-\text{SCH}_2\text{C}(\text{O})\text{CH}_2\text{CH}_3$ and $-\text{SCH}_2\text{C}(\text{O})\text{C}(\text{CH}_3)_3$ thiolate groups respectively. The crystal structure of **1d**· $(\text{PF}_6)_2$ is shown in Fig. 5, with selected bond lengths and angles in Table 2. The structure adopted *syn* conformation, an arrangement which minimizes steric interactions between the thiolate ligands with the bulky terminal PPh_3 ligands. The dihedral angle between the two PtS_2 planes is 158.56° . The carbonyl groups are positioned above the two platinum atoms at a distance of $[\text{Pt}(1)\cdots\text{O}(2)]$ 2.839 Å and $[\text{Pt}(2)\cdots\text{O}(1)]$ 2.877 Å. The sum of the van der Waals radii for Pt and O is 3.24 Å [36], so they are close enough to indicate a weak donor interaction. The IR spectra of **1d**· $(\text{PF}_6)_2$ showed absorption peaks at 1713 cm^{-1} assigned to the incorporated carbonyl groups.

Fig. 3 shows the ESI-MS profile of the reaction of $[\text{Pt}_2(\mu\text{-S})_2(\text{PPh}_3)_4]$ **1** with $\text{BrCH}_2\text{C}(\text{O})\text{C}(\text{O})\text{CH}_2\text{Br}$, **c**. The reaction was shown by PSI-ESI-MS to be very fast. The time between formation of the monoalkylated derivative $[\text{Pt}_2(\mu\text{-S})(\mu\text{-SCH}_2\text{C}(\text{O})\text{C}(\text{O})\text{CH}_2\text{Br})(\text{PPh}_3)_4]^+$, **1e** and the expected bridging dialkylated derivative



Scheme 1. Alkylation reactions of $[\text{Pt}_2(\mu\text{-S})_2(\text{PPh}_3)_4]$ (**1**) with reactive α -bromoketones alkylating agents, $\text{BrCH}_2\text{C}(\text{O})\text{C}(\text{CH}_3)_3$ (**a**), $\text{BrCH}_2\text{C}(\text{O})\text{CH}_2\text{CH}_3$ (**b**), and diketone, $\text{BrCH}_2\text{C}(\text{O})\text{C}(\text{O})\text{CH}_2\text{Br}$ (**c**).

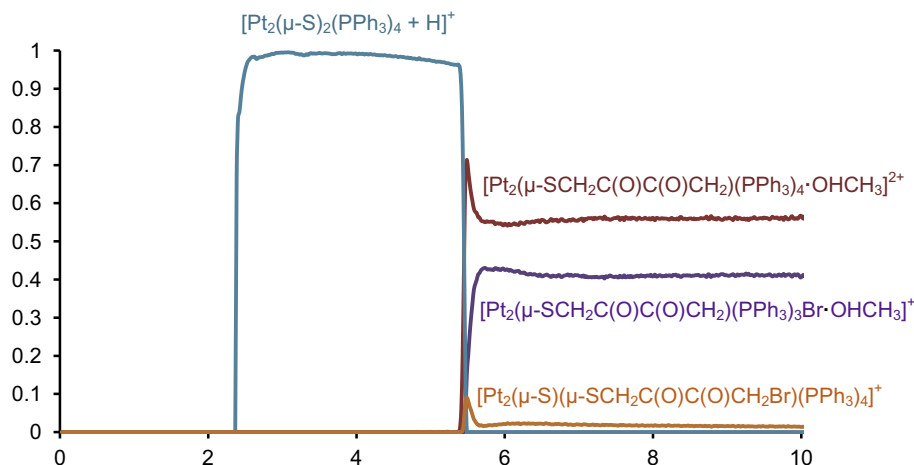


Fig. 3. The profile of the reaction of $[\text{Pt}_2(\mu\text{-S})_2(\text{PPh}_3)_4]$ **1** (injected at 2.4 min) with an excess of $\text{BrCH}_2\text{C}(\text{O})\text{C}(\text{O})\text{CH}_2\text{Br}$, **c** (injected at 5.5 min) to form first the $[\text{Pt}_2(\mu\text{-S})(\mu\text{-SCH}_2\text{C}(\text{O})\text{C}(\text{O})\text{CH}_2\text{Br})(\text{PPh}_3)_4\text{-OHCH}_3]^{2+}$, **1e** monocation then the intramolecular bridged dication $[\text{Pt}_2(\mu\text{-SCH}_2\text{C}(\text{O})\text{C}(\text{O})\text{CH}_2\text{S})(\text{PPh}_3)_3\text{-OHCH}_3]^{2+}$, **1g**. Another product $[\text{Pt}_2(\mu\text{-SCH}_2\text{C}(\text{O})\text{C}(\text{O})\text{CH}_2\text{S})(\text{PPh}_3)_3\text{Br-OHCH}_3]^+$, **1h** in which Br^- had replaced a PPh_3 ligand also appeared.

$[\text{Pt}_2(\mu\text{-SCH}_2\text{C}(\text{O})\text{C}(\text{O})\text{CH}_2\text{S})(\text{PPh}_3)_4]^{2+}$, **1f** is less than two seconds. Kinetic plots from the ESI-MS reaction profile data of the mono- and dialkylation reactions show they are both first order. The reaction profile shows two species, at $m/z = 809.6$ and 1436.8 compared with the expected mass $m/z = 795$ (ca) of the product **1f**. The ESI-MS of the isolated product from the bench top synthesis showed only a peak at $m/z = 809.6$. This species was tentatively assigned to the methanol adduct, $[\text{Pt}_2(\mu\text{-SCH}_2\text{C}(\text{O})\text{C}(\text{O})\text{CH}_2\text{S})(\text{PPh}_3)_4\text{-OHCH}_3]^{2+}$, **1g** formed immediately upon formation of **1f**.

Formation of this type of methanol adduct has earlier been observed under ESI-MS conditions for the reaction of α,ω -monoketone electrophile, $\text{ClCH}_2\text{C}(\text{O})\text{CH}_2\text{Cl}$ with **1** [30]. The peak of a cation at $m/z = 1436.8$ is attributable to $[\text{Pt}_2(\mu\text{-SCH}_2\text{C}(\text{O})\text{C}(\text{O})\text{CH}_2\text{S})(\text{PPh}_3)_3\text{Br-OHCH}_3]^+$, **1h** formed from the displacement of a PPh_3 by the Br^- leaving group. The masses were identified by comparing the high resolution mass spectral (HR-MS) isotope patterns with calculated isotope patterns [37]. Attempts at obtaining suitable single crystals of the products as the $[\text{PF}_6]^-$ salt were unsuccessful.

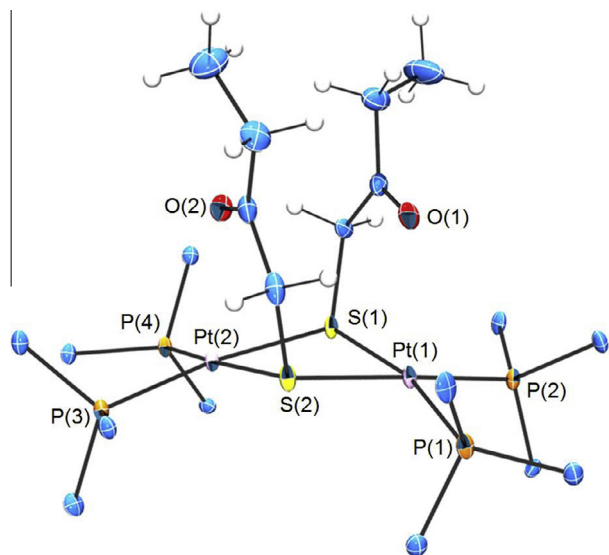


Fig. 4. Molecular structure of the core of the complex $[\text{Pt}_2(\mu\text{-SCH}_2\text{C}(\text{O})\text{CH}_2\text{CH}_3)_2(\text{PPh}_3)_4]^{2+}$, **1c**, with only the ipso carbon atoms of the PPh_3 ligands shown.

Table 1
Selected bond lengths (Å) and angles (°) for $[\text{Pt}_2(\mu\text{-SCH}_2\text{C}(\text{O})\text{CH}_2\text{CH}_3)_2(\text{PPh}_3)_4]^{2+}$, **1c**.

Bond lengths and atomic distances (Å)			
Pt(1)–P(1)	2.292(2)	Pt(1)–P(2)	2.285(2)
Pt(2)–P(3)	2.286(2)	Pt(2)–P(4)	2.2951(19)
Pt(1)–S(1)	2.3570(19)	Pt(1)–S(2)	2.375(2)
Pt(2)–S(1)	2.3863(19)	Pt(2)–S(2)	2.354(2)
S(1)–C(1)	1.796(9)	S(2)–C(5)	1.806(10)
C(1)–C(2)	1.520(11)	C(5)–C(6)	1.535(14)
O(1)–C(2)	1.218(11)	O(2)–C(6)	1.205(11)
C(2)–C(3)	1.507(14)	C(6)–C(7)	1.490(13)
C(3)–C(4)	1.494(17)	C(7)–C(8)	1.532(17)
Bond angles (°)			
P(1)–Pt(1)–S(2)	86.84(7)	P(2)–Pt(1)–S(1)	93.40(7)
P(4)–Pt(2)–S(1)	88.17(7)	P(3)–Pt(2)–S(2)	92.53(7)
S(1)–Pt(1)–S(2)	81.75(7)	S(2)–Pt(2)–S(1)	81.57(7)
C(1)–S(1)–Pt(1)	107.9(3)	C(5)–S(2)–Pt(1)	111.6(3)
C(1)–S(1)–Pt(2)	111.7(3)	C(5)–S(2)–Pt(2)	107.8(3)
Pt(2)–S(2)–Pt(1)	96.50(7)	Pt(1)–S(1)–Pt(2)	96.11(7)
C(2)–C(1)–S(1)	120.0(6)	C(6)–C(5)–S(2)	121.3(6)
O(1)–C(2)–C(1)	122.7(8)	O(2)–C(6)–C(5)	122.7(8)
O(1)–C(2)–C(3)	121.9(8)	O(2)–C(6)–C(7)	124.5(10)
C(4)–C(3)–C(2)	113.6(10)	C(6)–C(7)–C(8)	112.7(9)

The corresponding tetraphenylborate complex **1f**(BPh_4)₂ dried under vacuum overnight did however yield suitable crystals for X-ray structure determination. The structure of the dication is shown in Fig. 6 and the selected bond lengths and angles in Table 3. The $^{31}\text{P}\{^1\text{H}\}$ NMR spectrum of **1f**(PF_6)₂ showed a single resonance at δ 19.62 showing $^1\text{J}(\text{PtP})$ 3021 Hz, consistent with a highly symmetric structure of the complex. In the ^1H NMR spectrum, a broad resonance at δ 3.50 is assigned to the SCH_2 protons, and the complicated signals at the phenyl region indicated formation of **1f**. The IR spectra showed absorption peaks that confirmed the formation of **1f**(PF_6)₂ with a double peak at 1711 cm^{-1} characteristic of the carbonyls of the diketone ($-\text{CH}_2\text{C}(\text{O})\text{C}(\text{O})\text{CH}_2-$) of the incorporated group.

3. Experimental

3.1. Materials and instrumentation

The alkylating agents $\text{BrCH}_2\text{C}(\text{O})\text{C}(\text{CH}_3)_3$, $\text{BrCH}_2\text{C}(\text{O})\text{CH}_2\text{CH}_3$ and $\text{BrCH}_2\text{C}(\text{O})\text{C}(\text{O})\text{CH}_2\text{Br}$ were supplied by Alfa Aesar; CAUTION!:-

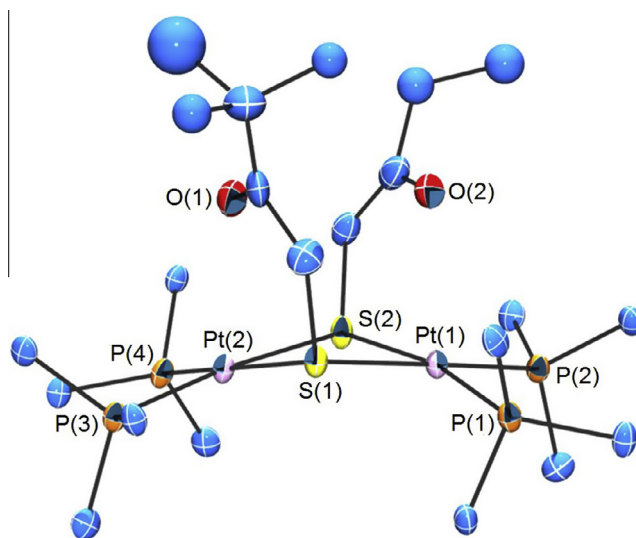


Fig. 5. Molecular structure of the core of the complex $[\text{Pt}_2(\mu\text{-SCH}_2\text{C}(\text{O})\text{CH}_2\text{CH}_3)(\text{CH}_3)_3(\mu\text{-SCH}_2\text{C}(\text{O})\text{CH}_2\text{CH}_3)(\text{PPh}_3)_4]^{2+}$, **1d**, with only the ipso carbon atoms of the PPh_3 ligands shown.

Table 2
Selected bond lengths (Å) and angles (°) for $[\text{Pt}_2\{\mu\text{-SCH}_2\text{C}(\text{O})\text{C}(\text{CH}_3)_3\}\{\mu\text{-SCH}_2\text{C}(\text{O})\text{CH}_2\text{CH}_3\}(\text{PPh}_3)_4]^{2+}$, **1d**.

Bond lengths and atomic distances (Å)			
Pt(1)–P(1)	2.2864(18)	Pt(1)–P(2)	2.2847(19)
Pt(2)–P(3)	2.2784(19)	Pt(2)–P(4)	2.2904(19)
Pt(1)–S(1)	2.3678(18)	Pt(1)–S(2)	2.3534(18)
Pt(2)–S(1)	2.3627(17)	Pt(2)–S(2)	2.3822(18)
S(1)–C(1)	1.806(8)	S(2)–C(7)	1.797(8)
C(1)–C(2)	1.508(11)	C(7)–C(8)	1.505(12)
O(1)–C(2)	1.196(10)	O(2)–C(8)	1.207(10)
C(2)–C(3)	1.513(12)	C(8)–C(9)	1.520(13)
Bond angles (°)			
P(1)–Pt(1)–S(2)	166.14(6)	P(2)–Pt(1)–S(1)	174.49(6)
P(4)–Pt(2)–S(1)	169.17(6)	P(3)–Pt(2)–S(2)	172.76(6)
S(1)–Pt(1)–S(2)	82.06(6)	S(2)–Pt(2)–S(1)	81.59(6)
C(1)–S(1)–Pt(1)	109.5(3)	C(7)–S(2)–Pt(1)	109.3(3)
C(1)–S(1)–Pt(2)	108.4(3)	C(7)–S(2)–Pt(2)	112.3(3)
Pt(2)–S(2)–Pt(1)	95.83(6)	Pt(1)–S(1)–Pt(2)	96.97(6)
C(2)–C(1)–S(1)	121.3(6)	C(8)–C(7)–S(2)	119.7(6)
O(1)–C(2)–C(1)	122.6(7)	O(2)–C(8)–C(7)	124.6(7)
O(1)–C(2)–C(3)	120.8(8)	O(2)–C(8)–C(9)	127.9(11)

highly toxic, potent lachrymator and vesicant and should be handled using appropriate safety precautions. *Cis*- $\text{PtCl}_2(\text{PPh}_3)_2$, $\text{Na}_2\text{S}\cdot 9\text{H}_2\text{O}$, NH_4PF_6 and NaBPh_4 were supplied by Sigma–Aldrich. Reaction solvents: benzene (Sigma–Aldrich), methanol (Caledon Laboratories), dichloromethane (Sigma–Aldrich) and diethyl ether (EMD Chemicals) were reagent grade and used without further purification. $[\text{Pt}_2(\mu\text{-S})_2(\text{PPh}_3)_4]$ **1** was synthesised according to a reported literature procedure by the metathesis reaction of *cis*- $\text{PtCl}_2(\text{PPh}_3)_2$ with $\text{Na}_2\text{S}\cdot 9\text{H}_2\text{O}$ in benzene [17,38].

Elemental analyses were performed on a Perkin–Elmer 2400 CHN elemental analyzer. NMR spectra were recorded in CDCl_3 solution, unless otherwise stated. ^1H and $^{31}\text{P}\{^1\text{H}\}$ spectra referenced to TMS for ^1H and 85% phosphoric acid for ^{31}P were recorded on a Bruker DRX 300 MHz spectrometer. IR spectra were obtained as KBr disks with a Perkin Elmer Spectrum FTIR spectrometer, version 10.4.3. Melting points of the compounds were determined with a Galenkamp melting point apparatus in air and uncorrected. ESI–MS of solid products were obtained by dissolving a small quantity of the material in 1–2 drops of dichloromethane, followed by dilution to

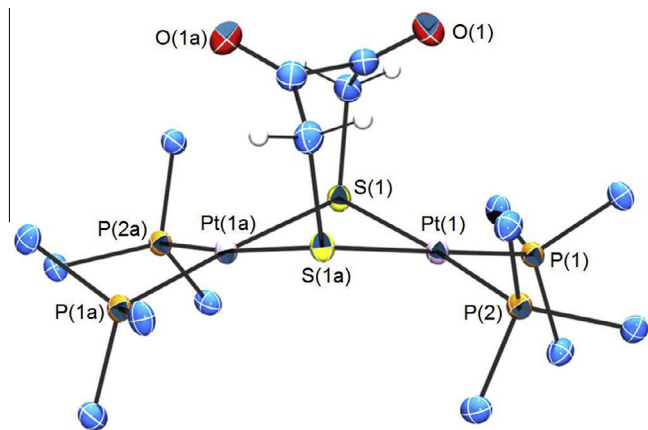


Fig. 6. Molecular structure of the core of the complex $[\text{Pt}_2\{\mu\text{-SCH}_2\text{C}(\text{O})\text{C}(\text{O})\text{CH}_2\text{S}\}(\text{PPh}_3)_4]^{2+}$, **1f**, with only the ipso carbon atoms of the PPh_3 ligands shown.

Table 3
Selected bond lengths (Å) and angles ($^\circ$) for $[\text{Pt}_2\{\mu\text{-SCH}_2\text{C}(\text{O})\text{C}(\text{O})\text{CH}_2\text{S}\}(\text{PPh}_3)_4]^{2+}$, **1f**.

Bond lengths and atomic distances (Å)			
Pt(1)–P(1)	2.2940(7)	Pt(1)–P(2)	2.3054(7)
Pt(1)–S(1a)	2.3837(7)	Pt(1)–S(1)	2.3589(7)
S(1)–C(1)	1.838(3)	Pt(1a)–S(1)	2.3837(7)
C(1)–C(2)	1.501(4)	C(2)–O(1)	1.207(3)
C(2)–C(2a)	1.534(5)		
Bond angles ($^\circ$)			
P(1)–Pt(1)–P(2)	98.98(2)	P(1)–Pt(1)–S(1)	92.54(2)
P(2)–Pt(1)–S(1)	168.48(2)	P(1)–Pt(1)–S(1a)	174.89(2)
P(2)–Pt(1)–S(1a)	85.93(2)	S(1)–Pt(1)–S(1a)	82.57(2)
C(1)–S(1)–Pt(1)	103.85(9)	C(1)–S(1)–Pt(1a)	111.04(9)
Pt(1)–S(1)–Pt(1a)	92.46(2)	C(2)–C(1)–S(1)	111.12(18)
O(1)–C(2)–C(2a)	119.2(3)	O(1)–C(2)–C(1)	124.7(3)
C(1)–C(2)–C(2a)	116.1(3)		

ca. 2 mL using methanol. All mass spectra were collected on a Waters Micromass Q-TOF II Micro mass spectrometer in positive ion mode, using electrospray ionization: capillary voltage, 3.0 kV; source cone, 20 V; extraction cone, 1 V; source temperature, 80 $^\circ\text{C}$; desolvation temperature, 160 $^\circ\text{C}$; cone gas flow, 100 L/h; desolvation gas flow, 200 L/h; collision voltage for MS experiments 5 V and 5–40 V for MS/MS experiments; MCP voltage, 2100 V. No smoothing of the data was performed and comparison of observed and calculated isotope patterns [37] was used to assist ion assignment.

3.2. Pressurised Sample Infusion-Electrospray Ionization-Mass Spectrometry (PSI-ESI-MS) procedure

The kinetic profiles of the reactions were analyzed by PSI-ESI-MS. $[\text{Pt}_2(\mu\text{-S})_2(\text{PPh}_3)_4]$ **1** (6.0 mg) and excess amount of each of the electrophiles $\text{BrCH}_2\text{C}(\text{O})\text{C}(\text{CH}_3)_3$ (**a**), (ca 0.1 mL), $\text{BrCH}_2\text{C}(\text{O})\text{CH}_2\text{CH}_3$ (**b**), (ca 0.1 mL) and $\text{BrCH}_2\text{C}(\text{O})\text{C}(\text{O})\text{CH}_2\text{Br}$ (**c**), (0.023 mg) were used in the experiments. The reaction solvent (methanol, 10 mL) was sparged with nitrogen on the Schlenk line to remove oxygen. **1** was added to the Schlenk flask. PEEK tubing was inserted through a septum into the reaction mixture solution, with the other end connected to the ESI-MS source. The methanolic solution of **1** was driven into ESI-MS using an overpressure using 2 psi argon. As soon as the signal for $[\mathbf{1}+\text{H}]^+$ at m/z 1503.5 reached a stable intensity, 1 mL methanol solution of the alkylating agent was injected by syringe through the septum into the reaction mixture to initiate the reaction. Spectra were recorded once per second to generate the abundance versus time data.

3.3. Syntheses of the alkylated complexes

3.3.1. Synthesis of $[\text{Pt}_2(\mu\text{-S})\{\mu\text{-CH}_2\text{C}(\text{O})\text{C}(\text{CH}_3)_3\}(\text{PPh}_3)_4](\text{BPh}_4)$, **1a** (BPh_4)

To a suspension of $[\text{Pt}_2(\mu\text{-S})_2(\text{PPh}_3)_4]$ (50 mg, 0.033 mmol) in methanol (25 mL) was added large excess of $\text{BrCH}_2\text{C}(\text{O})\text{C}(\text{CH}_3)_3$ (0.1 mL, 0.74 mmol, 22.4 mol equiv.) and solution stirred for 20 min at room temperature. Complete formation of the monoalkylated product was confirmed by ESI-MS which showed $[\text{Pt}_2(\mu\text{-S})(\mu\text{-SCH}_2\text{C}(\text{O})\text{C}(\text{CH}_3)_3)(\text{PPh}_3)_4]^+$ at m/z 1603.93. The solution was filtered and NaBPh_4 (25.04 mg, 0.16 mmol) added to the clear filtrate. The resulting yellow precipitates were filtered, washed with water (4×10 mL) and diethyl ether (4×10 mL) and dried in air, giving **1a** (BPh_4) (54 mg, 85%). M.p. 122–124 $^\circ\text{C}$; *Anal. Calc.* for $\text{C}_{102}\text{H}_{91}\text{BOP}_4\text{Pt}_2\text{S}_2$ (Mr. 1921.82): C, 63.6; H, 5.0. Found: C, 63.8; H, 4.8%. IR ν_{max} 1096, 1435, 1480, 1580, 1708, 2983, 3054 cm^{-1} ; ^1H NMR (CDCl_3 , 300 MHz), δ 6.87–7.51 (85H, m, 17Ph), 3.48 [2H, t, SCH_2 , $^3J(\text{PtH})$ 34.65, $^4J(\text{PH})$ 3.56]; $^{31}\text{P}\{^1\text{H}\}$ NMR, (CDCl_3) δ 23.39 [d, $^1J(\text{PtP}_B)$ 3376.47, PB], 23.9 [d, $^1J(\text{PtP}_A)$ 2653.35, PA]; ESI-MS, (MeOH) 20 V: m/z (%) 1603.9 ($[\text{M}]^+$ 100).

3.3.2. Synthesis of $[\text{Pt}_2\{\mu\text{-SCH}_2\text{C}(\text{O})\text{CH}_2\text{CH}_3\}_2(\text{PPh}_3)_4](\text{PF}_6)_2$, **1c** (PF_6)₂

To a stirred suspension of $[\text{Pt}_2(\mu\text{-S})_2(\text{PPh}_3)_4]$ (50 mg, 0.033 mmol) in methanol (25 mL) was added $\text{BrCH}_2\text{C}(\text{O})\text{CH}_2\text{CH}_3$ (0.1 mL, 0.98 mmol, ≈ 30 mol equiv.). The solution was stirred for 2 h at room temperature. Complete formation of the product was confirmed by ESI-MS which showed $[\text{Pt}_2\{\mu\text{-SCH}_2\text{C}(\text{O})\text{CH}_2\text{CH}_3\}_2(\text{PPh}_3)_4]^{2+}$ at m/z 821.58. The solution was filtered and NH_4PF_6 (25.04 mg, 0.16 mmol) added to the clear, colorless filtrate. The resulting precipitate was filtered, washed with water (4×10 mL) and diethyl ether (4×10 mL) and dried, giving **1c** (PF_6)₂ (44 mg, 68%) as a white solid. Crystals suitable for X-ray crystallography were isolated by vapour diffusion of diethyl ether into a dichloromethane solution of **1c** (PF_6)₂. M.p. 163–165 $^\circ\text{C}$; *Anal. Calc.* for $\text{C}_{80}\text{H}_{74}\text{F}_{12}\text{O}_2\text{P}_6\text{Pt}_2\text{S}_2$ (Mr. 1935.56): C, 49.5; H, 4.1. Found: C, 49.8; H, 4.1%. IR ν_{max} 1098, 1437, 1483, 1712, 3057 cm^{-1} ; ^1H NMR (CDCl_3 , 300 MHz), δ 2.58 (br s, 4H, S–CH₂), 0.72 (tr, 6H, CH₃), 1.88 (qt, 4H, CH₂), 7.17–7.35 (m, 60H, Ph); $^{31}\text{P}\{^1\text{H}\}$ NMR (121.5 MHz, CDCl_3), δ 19.17 [s, $^1J(\text{PtP})$ 3059]; ESI-MS, (MeOH) 20 V: m/z (%) 821.6 ($[\text{M}]^{2+}$ 100%).

3.3.3. Synthesis of $[\text{Pt}_2\{\mu\text{-SCH}_2\text{C}(\text{O})\text{C}(\text{CH}_3)_3\}\{\mu\text{-SCH}_2\text{C}(\text{O})\text{CH}_2\text{CH}_3\}(\text{PPh}_3)_4](\text{PF}_6)_2$, **1d** (PF_6)₂

To a stirred suspension of $[\text{Pt}_2(\mu\text{-S})_2(\text{PPh}_3)_4]$ (50 mg, 0.033 mmol) in methanol (25 mL) was added $\text{BrCH}_2\text{C}(\text{O})\text{CH}_2(\text{CH}_3)_3$ (0.1 mL, 0.98 mmol, ≈ 30 mol equiv.). The solution was stirred for 20 min at room temperature. Complete formation of the monoalkylated product was confirmed by ESI-MS which showed $[\text{Pt}_2(\mu\text{-S})\{\mu\text{-SCH}_2\text{C}(\text{O})\text{CH}_2(\text{CH}_3)_3\}(\text{PPh}_3)_4]^{2+}$ at m/z 1601.93. Excess $\text{BrCH}_2\text{C}(\text{O})\text{CH}_2\text{CH}_3$ (0.1 mL, 0.98 mmol) was added to the reaction mixture and stirred for 1 h. Complete formation of the heteroalkylated derivative $[\text{Pt}_2\{\mu\text{-SCH}_2\text{C}(\text{O})\text{C}(\text{CH}_3)_3\}\{\mu\text{-SCH}_2\text{C}(\text{O})\text{CH}_2\text{CH}_3\}(\text{PPh}_3)_4]^+$ was confirmed by ESI-MS which showed a m/z at 836.79. The solution was gravity filtered and NH_4PF_6 (25.04 mg, 0.16 mmol) added to the clear, colorless filtrate. The resulting precipitate was filtered, washed with water (4×10 mL) and diethyl ether (4×10 mL) and dried over vacuum, giving **1d** (PF_6)₂ (44 mg, 68%) as white solids. Crystals suitable for X-ray crystallography were isolated by vapour diffusion of diethyl ether into a dichloromethane solution **1d** (PF_6)₂. M.p. 172–174 $^\circ\text{C}$; *Anal. Calc.* for $\text{C}_{82}\text{H}_{78}\text{F}_{12}\text{O}_2\text{P}_6\text{Pt}_2\text{S}_2$ (Mr. 1963.62): C, 50.1; H, 4.2. Found: C, 50.6; H, 4.2%. IR ν_{max} 1097, 1437, 1483, 1713, 3059 cm^{-1} ; ^1H NMR (300 MHz, CDCl_3), δ 0.78 (br s, 3H, CH₃), 1.82 (qt m, 2H, CH₂), 2.26 (br s, 2H, CH₂), 2.44 (br s, 2H, CH₂), 7.04–7.49 (m, 60H, Ph); $^{31}\text{P}\{^1\text{H}\}$ NMR (121.5 MHz, CDCl_3) δ 18.65 [m, $^1J(\text{PtP})$ 3086], 19.28 [m, $^1J(\text{PtP})$ 3086]; ESI-MS, (MeOH) 20 V: m/z (%) 836.8 ($[\text{M}]^{2+}$ 100%).

Table 4
Crystallographic data for complexes **1c**·(PF₆)₂, **1d**·(PF₆)₂ and **1f**·(BPh₄)₂.

Identification code	1c ·(PF ₆) ₂ ·3CH ₂ Cl ₂	1d ·(PF ₆) ₂ ·3CH ₂ Cl ₂	1f ·(BPh ₄) ₂
Formula	C ₈₃ H ₈₀ Cl ₆ F ₁₂ O ₂ P ₆ Pt ₂ S ₂	C _{84.19} H _{82.39} Cl _{4.39} F ₁₂ O ₂ P ₆ Pt ₂ S ₂	C ₁₂₈ H ₁₁₄ B ₂ O ₃ P ₄ Pt ₂ S ₂
Formula weight	2190.29	2149.97	2299.99
T (K)	120(2)	120(2)	120(2)
λ (Å)	0.71073	0.71073	0.71073
Crystal system	triclinic	monoclinic	monoclinic
Space group	P $\bar{1}$	P2 ₁ /n	C2/c
Unit cell dimensions	a = 13.4440(15) Å, α = 86.265(2)° b = 17.5218(19) Å, β = 81.410(2)° c = 18.331(2) Å, γ = 87.858(2)°	a = 17.3992(10) Å, α = 90° b = 23.2587(14) Å, β = 92.328(2)° c = 21.1180(13) Å, γ = 90°	a = 31.745(4) Å, α = 90° b = 14.6486(17) Å, β = 115.810(4)° c = 27.674(4) Å, γ = 90°
V (Å ³)	4258.9(8)	8539.0(9)	11585(3)
Z	2	4	4
Density (calculated) (g cm ⁻³)	1.708	1.672	1.319
Absorption coefficient (μ) (mm ⁻¹)	3.704	3.645	2.554
F(000)	2164	4257	4656
Crystal color, habit	Colorless, rod	Colorless, block	Colorless, block
Crystal size (mm ³)	0.114 × 0.062 × 0.041	0.080 × 0.060 × 0.054	0.510 × 0.229 × 0.114
θ range for data collection	1.165–27.337°		1.425–27.298°
Index ranges	–17 ≤ h ≤ 17, –22 ≤ k ≤ 22, –23 ≤ l ≤ 23	–21 ≤ h ≤ 21, –29 ≤ k ≤ 20, –26 ≤ l ≤ 26	–40 ≤ h ≤ 40, –18 ≤ k ≤ 18, –35 ≤ l ≤ 35
Reflections collected	88400	137757	119881
Independent reflections (R _{int})	19160 (0.0565)	17853 (0.1098)	13007 (0.0293)
Completeness to θ = 25.242°	100.0%	100.0%	99.9%
Absorption correction	Numerical	Numerical	Numerical
Max. and min. transmission	0.9314 and 0.7508	0.9901 and 0.8015	0.8156 and 0.4016
Refinement method	Full-matrix least-squares on F ²	Full-matrix least-squares on F ²	Full-matrix least-squares on F ²
Data/restraints/parameters	19160/0/1020	17853/11/1018	13007/3/658
Goodness-of-fit (GOF) on F ²	1.144	1.023	1.062
Final R indices [I > 2σ(I)]	R ₁ = 0.0617, wR ₂ = 0.1359	R ₁ = 0.0487, wR ₂ = 0.1063	R ₁ = 0.0252, wR ₂ = 0.0636
R indices (all data)	R ₁ = 0.0802, wR ₂ = 0.1432	R ₁ = 0.0857, wR ₂ = 0.1215	R ₁ = 0.0304, wR ₂ = 0.0672
Extinction coefficient	n/a	n/a	n/a
Largest difference peak and hole (e ⁻ Å ⁻³)	4.670 and –2.895	2.983 and –1.561	2.642 and –0.730

3.3.4. Synthesis of [Pt₂{μ-SCH₂C(O)C(O)CH₂S}(PPh₃)₄](PF₆)₂, **1f**·(PF₆)₂

A suspension of [Pt₂(μ-S)₂(PPh₃)₄] (50 mg, 0.033 mmol) and BrCH₂C(O)C(O)CH₂Br (0.0081 mg, 0.033 mmol) in methanol (25 mL) was stirred for 25 min at room temperature. Complete formation of a cyclized product was confirmed by ESI-MS which showed a single peak of the methanol adduct, [Pt₂{μ-SCH₂C(O)C(O)CH₂S}(PPh₃)₄-OHCH₃]²⁺ at m/z = 809.6. The solution was filtered and NH₄PF₆ (25.04 mg, 0.16 mmol) was added to the clear, colourless filtrate. The resulting white precipitate was filtered, washed repeatedly with distilled water (4 × 10 mL) and diethyl ether (4 × 10 mL), dried in air and under vacuum, giving **1f**·(PF₆)₂ (46 mg, 73%) as a white solid. Crystals of the [BPh₄]⁻ salt, **1f**·(BPh₄)₂ suitable for X-ray crystallography were isolated by vapour diffusion of diethyl ether into the dichloromethane solution. M.p. 153–155 °C; Anal. Calc. for C₁₂₄H₁₀₄B₂O₂P₄Pt₂S₂ (Mr. 2225.97): C, 66.8; H, 4.9. Found: C, 67.4; H, 4.8%. IR ν_{max} 1096, 1436, 1481, 1580 1619, 1711, 3054 cm⁻¹; ¹H NMR (CDCl₃, 300 MHz) δ 3.50 (br s, 4H, CH₂), 7.01–7.59 (m, 80H, Ph); ³¹P{¹H} NMR (CDCl₃) δ 19.62 [s, ¹(PtP) 3016]; ESI-MS, (MeOH) 20 V: m/z (%) 809.6 ([M]²⁺ 100).

3.4. X-ray crystal structure determinations

An appropriately sized crystal, having approximate dimensions of 0.114 × 0.062 × 0.041 mm, **1c**·(PF₆)₂; 0.080 × 0.060 × 0.054 mm **1d**·(PF₆)₂; and 0.510 × 0.229 × 0.114 mm, **1f**·(BPh₄)₂ was selected from each bulk sample under Paratone-N oil and mounted on a MiTeGen loop. The loop was transferred to a Bruker APEX-II diffractometer equipped with a CCD area detector under a cold gaseous nitrogen stream. An arbitrary sphere of data was recorded, using Mo Kα radiation (λ 0.71073 Å) and combination of ω- and φ-scans of 0.5° [39]. Data were corrected for absorption and polar-

ization effects and analyzed for space group determination. The structure was solved by intrinsic phasing methods and expanded routinely [40]. The model was refined by full-matrix least-squares analysis of F² against all reflections [41]. All non-hydrogen atoms were refined with anisotropic thermal displacement parameters. Unless otherwise noted, hydrogen atoms were included in calculated positions. Thermal parameters for the hydrogens were tied to the isotropic thermal parameter of the atom to which they are bonded (1.5 U_{eq}(C) for methyl, 1.2 U_{eq}(C) for all others). Crystallographic data are summarised in Table 4.

3.4.1. [Pt₂{μ-SCH₂C(O)CH₂CH₂S}(PPh₃)₄]²⁺, **1c**·(PF₆)₂·3CH₂Cl₂

1c·(PF₆)₂·3CH₂Cl₂ crystallized as colourless rod-like crystals. There are two molecules of the platinum-containing dication, four molecules of the associated [PF₆]⁻ anion and six molecules of dichloromethane of crystallization in the unit cell of the primitive, centrosymmetric, triclinic space group P $\bar{1}$. The structure of the cation is as expected. The complex consists of two Pt centers, each coordinated in a four-coordinate square planar fashion by two triphenyl phosphine ligands and two sulfurs of the bridging thio-late moieties. There is residual electron density near the Pt centers. Successive attempts to improve the data through re-integration and absorption correction could not improve these Fourier peaks. The fold angle formed by the two coordination planes about the Pt centers is: 26.82(6)°. The two mercaptopentanone chains are oriented in a *syn* fashion.

3.4.2. [Pt₂{μ-SCH₂C(O)C(CH₃)₃}{μ-SCH₂C(O)CH₂CH₃}(PPh₃)₄](PF₆)₂, **1d**·(PF₆)₂·3CH₂Cl₂

The complex crystallized as colorless block-like crystals from a vapour diffusion of diethyl ether into the dichloromethane solution. There is one molecule of the di-platinum dication and two

molecules of $[\text{PF}_6]^-$ anion in the asymmetric unit of the primitive, centrosymmetric, monoclinic space group $P2_1/n$. Also within the asymmetric unit are three disordered dichloromethane molecules.

The dication consists of two Pt centers, each coordinated in a slightly distorted four-coordinate, square planar fashion by two triphenylphosphine ligands and the two bridging sulfur atoms of the two thiolate ligands (Fig. 5 and Table 2). Bond distances about the Pt centers are unexceptional.

There is disorder of the thiolate ligands within the structure. The ratio was modeled as 0.6:0.4 at each site. Thus, 60% of the time the *t*-Bu and ethyl chain are in one position and the remaining 40% their positions are reversed (with respect to, for example, S1). The disorder was observed clearly in the major component where the terminal carbon of the ethyl chain was misoriented with respect to the *t*-Bu group that it overlays. The disorder for the minor component was readily observed for the *t*-Bu group (C10A–C12A), however, the ethyl group was found to overlap with C6 fairly closely. Only the slightly exaggerated atomic displacement ellipsoid of that atom indicated its likely position. Mild bond distance and angle restraints were applied to the model to retain a reasonable geometry to the disordered components. All of the disordered *t*-Bu/ethyl carbon atoms were refined with isotropic displacement parameters.

In addition to the salt, there are one full occupancy and two partial occupancy dichloromethane molecules of crystallization. All three are located within a channel within the lattice. Examination of residual electron density after modeling these solvent molecules indicates that there is likely considerable displacement of the solvent within this channel and the model here accounts for a reasonable estimate. Bond distance restraints were applied to sensibly model these disordered solvent molecules. The partially occupied solvent molecules were refined with independent site occupancy factors giving 0.75 and 0.45 at each site.

3.4.3. $[\text{Pt}_2\{\mu\text{-SCH}_2\text{C}(\text{O})\text{C}(\text{O})\text{CH}_2\text{S}\}(\text{PPh}_3)_4](\text{BPh}_4)_2$, **1f**(BPh_4)₂

The complex crystallizes as colorless block-like crystals from dichloromethane/diethyl ether. There are four molecules of the di-platinum di-cation, eight molecules of $[\text{BPh}_4]^-$ anion and four molecules of diethyl ether, disordered over two sites, in the unit cell of the C-centered, centrosymmetric, monoclinic space group $C2/c$.

The di-platinum cation consists of two Pt centers, each coordinated in a square-planar fashion by two *cis*-triphenylphosphine ligands and bridged by the two sulfur atoms of a 2,3-dioxobutane-1,4-bis(thiolate) anion (Fig. 6 and Tables 3). The cation resides on the crystallographic twofold axis at [0.5, *y*, 0.25], thus only half of the cation is represented in the asymmetric unit. The $[\text{BPh}_4]^-$ anion resides in a general position.

The ether of crystallization was modeled with half occupancy atoms to yield reasonable atomic displacement parameters. Also present in the initial model was diffuse, disorganized electron density that could not be reliably modeled as any particular molecular species. Application of the SQUEEZE routine in PLATON [42] showed the presence of four void spaces within the unit cell, each having a void volume of 253 Å³ and accounting for 42 e⁻ each. The intensity information for this density was corrected. This solvent content has not been included in the chemical formula because its identity is unknown. Bond distances and angles within the molecules are otherwise as expected.

4. Conclusions

The investigation has demonstrated the successful synthesis of novel mono- and homodi- and heterodi- and bridgingdi-alkylated derivatives of $[\text{Pt}_2(\mu\text{-S})_2(\text{PPh}_3)_4]$, **1** through the reaction of

bromoacyl alkylating agent with the high nucleophilicity of the μ -sulfido ligands. The inability of electrophile $\text{BrCH}_2\text{C}(\text{O})\text{C}(\text{CH}_3)_3$, **a** to double alkylate **1** but $\text{BrCH}_2\text{C}(\text{O})\text{CH}_2\text{CH}_3$, **b** strongly suggest that apart from the leaving group, there is a threshold of residual positive charge on the alkylating carbon that encourages the dialkylation. We plan to explore the coordination chemistry of the incorporated ketone groups towards other metal fragments. The ability of using the functionalized derivatives to access multi-metallic molecules may likely depend on moderating their reactivity towards metal centers. The use of PSI-ESI-MS for real time reaction visualization will be a productive technique in further investigation of the chemistry of this system.

Acknowledgments

J.S.M. thanks the Natural Sciences and Engineering Research Council (NSERC) of Canada, the Canada Foundation for Innovation (CFI), the British Columbia Knowledge Development Fund (BCKDF), and the University of Victoria for instrumentation and operational funding. O.T.U. thanks the University of Nigeria, Nsukka for a study leave to complete this work. Prof. William Henderson of the University of Waikato, Hamilton, New Zealand is thanked for the sample of $[\text{Pt}_2(\mu\text{-S})_2(\text{PPh}_3)_4]$ used in the kinetic experiments.

Appendix A. Supplementary material

CCDC 1431896, 1431897 and 1431898 contains the supplementary crystallographic data for **1c**, **1d**, and **1f**. These data can be obtained free of charge from The Cambridge Crystallographic Data Centre via www.ccdc.cam.ac.uk/data_request/cif. Supplementary data associated with this article can be found, in the online version, at <http://dx.doi.org/10.1016/j.ica.2016.05.022>.

References

- [1] S.-W.A. Fong, T.S.A. Hor, *J. Chem. Soc., Dalton Trans.* (1999) 639.
- [2] W. Henderson, T.S.A. Hor, *Inorg. Chim. Acta* 363 (2010) 1859.
- [3] W. Henderson, A.G. Oliver, *Inorg. Chim. Acta* 375 (2011) 248.
- [4] P. González-Duarte, A. Lledós, R. Mas-Ballesté, *Eur. J. Inorg. Chem.* (2004) 3585.
- [5] S.-W.A. Fong, T.S.A. Hor, W. Henderson, B.K. Nicholson, S. Gardyne, S.M. Devoy, *J. Organomet. Chem.* 679 (2003) 24.
- [6] S.-W.A. Fong, T.S.A. Hor, S.M. Devoy, B.A. Waugh, B.K. Nicholson, W. Henderson, *Inorg. Chim. Acta* 357 (2004) 2081.
- [7] R. Mas-Ballesté, W. Clegg, A. Lledós, P. González-Duarte, *Eur. J. Inorg. Chem.* (2004) 3223.
- [8] S.M. Devoy, W. Henderson, B.K. Nicholson, J. Fawcett, T.S.A. Hor, *Dalton Trans.* (2005) 2780.
- [9] B.C. White, D. Harrison, W. Henderson, B.K. Nicholson, T.S.A. Hor, *Inorg. Chim. Acta* 363 (2010) 2387.
- [10] S.-W.A. Fong, W.T. Yap, J.J. Vittal, W. Henderson, T.S.A. Hor, *J. Chem. Soc., Dalton Trans.* (2002) 1826.
- [11] A. Bencini, M. Di Vaira, R. Morassi, P. Stoppioni, F. Mele, *Polyhedron* 15 (1996) 2079.
- [12] J.S.L. Yeo, J.J. Vittal, W. Henderson, T.S.A. Hor, *Organometallics* 21 (2002) 2944.
- [13] V.W.-W. Yam, P.K.-Y. Yeung, K.-K. Cheung, *Angew. Chem., Int. Ed. Engl.* 35 (1996) 739.
- [14] V.W.-W. Yam, K.-L. Yu, E.C.-C. Cheng, P.K.-Y. Yeung, K.-K. Cheung, N. Zhu, *Chem.-Eur. J.* 8 (2002) 4122.
- [15] J. Li, T.S.A. Hor, *Dalton Trans.* (2008) 6619.
- [16] R.R. Gukathasan, R.H. Morris, A. Walker, *Can. J. Chem.* (1983) 2490.
- [17] R. Ugo, G. La Monica, S. Cenini, A. Segre, F. Conti, *J. Chem. Soc. (A)* (1971) 522.
- [18] W. Henderson, S.H. Chong, T.S.A. Hor, *Inorg. Chim. Acta* 359 (2006) 3440.
- [19] S.H. Chong, L.L. Koh, W. Henderson, T.S.A. Hor, *Chem. Asian J.* 1 (2006) 264.
- [20] R. Mas-Ballesté, M. Capdevila, P.A. Champkin, W. Clegg, R.A. Coxall, A. Lledós, C. Mégret, P. González-Duarte, *Inorg. Chem.* 41 (2002) 3218.
- [21] M. Zhou, C.F. Lam, K.F. Mok, P.-H. Leung, T.S.A. Hor, *J. Organomet. Chem.* 476 (1994) C32.
- [22] S.H. Chong, D.J. Young, T.S.A. Hor, *J. Organomet. Chem.* 691 (2006) 349.
- [23] O.T. Ujam, W. Henderson, B.K. Nicholson, T.S.A. Hor, *Inorg. Chim. Acta* 363 (2010) 3558.
- [24] W. Henderson, G.C. Saunders, T.S.A. Hor, *Inorg. Chim. Acta* 368 (2011) 6.
- [25] J. Li, F. Li, L.L. Koh, T.S.A. Hor, *Dalton Trans.* 39 (2010) 2441.
- [26] W. Henderson, B.K. Nicholson, S.M. Devoy, T.S.A. Hor, *Inorg. Chim. Acta* 361 (2008) 1908.
- [27] S.H. Chong, W. Henderson, T.S.A. Hor, *Dalton Trans.* (2007) 4008.

- [28] O.T. Ujam, W. Henderson, B.K. Nicholson, T.S.A. Hor, *Inorg. Chim. Acta* 376 (2011) 255.
- [29] W. Henderson, B.K. Nicholson, O.T. Ujam, *J. Coord. Chem.* 64 (2011) 2771.
- [30] O.T. Ujam, S.M. Devoy, W. Henderson, B.K. Nicholson, T.S.A. Hor, *Dalton Trans.* 41 (2012) 12773.
- [31] K.L. Vikse, Z. Ahmadi, J. Luo, N. van der Wal, K. Daze, N. Taylor, J.S. McIndoe, *Int. J. Mass Spectrom.* 8 (2012) 323.
- [32] W. Henderson, J.S. McIndoe, *Mass Spectrometry of Inorganic and Organometallic Compounds: Tools – Techniques – Tips*, Wiley-Interscience, 2005.
- [33] K.L. Vikse, Z. Ahmadi, C.C. Manning, D.A. Harrington, J.S. McIndoe, *International Edition* 50 (2011) 8304.
- [34] K.L. Vikse, M.P. Woods, J.S. McIndoe, *Organometallics* 29 (2010) 6615.
- [35] T.G. Appleton, H.C. Clark, L.E. Manzer, *Coord. Chem. Rev.* 10 (1973) 335.
- [36] Cambridge Structural Database <<http://www.ccdc.cam.ac.uk/products/csd/radii/>>.
- [37] L. Patiny, A. Borel, *J. Chem. Inf. Model.* 53 (2013) 1223.
- [38] W. Henderson, B.K. Thwaite, T.S.A. Hor, Nicholson, *Eur. J. Inorg. Chem.* (2008) 5119.
- [39] Bruker AXS, APEX-2. Bruker-Nonius AXS, Madison, Wisconsin, USA, pp. 8.
- [40] G.M. Sheldrick, *Acta Cryst. A* 64 (2008) 112.
- [41] G.M. Sheldrick, *Acta Cryst. C* 71 (2015) 3.
- [42] A.L. Spek, *Acta Cryst. D* 65 (2009) 148.